SIMULATION OF HEAD-TAIL INSTABILITY CAUSED BY ELECTRON CLOUD IN THE POSITRON RING AT PEP-II*

Yunhai Cai, SLAC, Stanford, CA 94309, USA

Abstract

The head-tail instability caused by an electron cloud in positron storage rings is studied numerically using a simple model. In the model, the positron beam is longitudinally divided into many slices that have a fixed transverse size. The centroid of each slice evolves dynamically according to the interaction with a two-dimensional electron cloud at a given azimuthal location in the ring and a six-dimensional lattice map. A sudden and huge increase of the projected beam size and the mode coupling in the dipole spectrum are observed in the simulation at the threshold of the instability. Even below the threshold, the vertical beam size increases along a bunch train that has 8.5 ns bunch spacing. Above the threshold, a positive chromaticity can damp down the centroid motion but has very little effect on the blowup of the beam size. The results of the simulation are consistent with many observations at PEP-II.

1 INTRODUCTION

The transverse couple-bunch instability caused by an electron cloud in a positron storage ring was first observed in the spectrum of coherent dipole oscillation in the KEK Photon Factory [1]. The photoelectron produced by the synchrotron radiation is proposed as the primary cause of the instability by Ohmi [2]. He has simulated the production of the photoelectron and showed that the effective wake field due to the electron cloud couples the dipole motion between bunches and hence causes the coupled bunch instability for the positron beam. This instability can be controlled by a strong bunch-by-bunch feedback as demonstrated in the Low Energy Ring (LER) of KEK-B and PEP-II.

However, even with suppressed dipole oscillations, the electron cloud still causes significant emittance growth as observed recently in KEK and PEP-II B-factories [3, 4]. The growth has been explained numerically as a result of head-tail instability caused by the electron cloud by Ohmi and Zimmermann [5]. Since there is no direct experimental confirmation of the proposed theory, it is important to continue the study to establish the link between theory and experiment.

In this paper, we first briefly describe the physics and approximation in the simulation in the section 2 and 3. Then we make a simulation in section 5 and 6 to identify the threshold of the instability both in terms of the emittance growth and mode coupling. In section 7 and 8, we simulate the emittance growth below and above the threshold. Finally, we make a summary of the whole investigation. The focus of the simulation is on the observable in the ring. Where possible, we will make a comparison between experimental observations and the simulation.

There are two main sources of electrons: photoelectrons generated from the synchrotron radiation and secondary electrons from the multipacting on the vacuum chamber. The detail of how the electron cloud is generated can be found in the work by Furman and Lambertson [6]. In this paper, the density and distribution of the electron cloud are treated as an initial input to the simulation. We will concentrate on how the positron beam interacts with the electron cloud once the electrons are generated and reach the saturation density.

2 BEAM AND ELECTRON CLOUD

For the beam and electron cloud, we use a simple simulation model introduced by Ohmi and Zimmermann [5]. In the model, the transverse distribution of the electron cloud is represented by N_m macro particles at a given azimuthal location s in the positron ring,

$$\rho_{\perp}^{e}(\vec{x}_e, \vec{v}_e; s) = \frac{1}{N_m}\sum_{n=1}^{N_m}\delta(\vec{x}_e - \vec{x_e}_n(s))\delta(\vec{v}_e - \vec{v_e}_n(s)),$$

where $\vec{x}_e$ and $\vec{v}_e$ are the transverse coordinate and velocity for the electrons. The distribution of the positron bunch is represented by N_s longitudinal macro slices as illustrated in Fig. 1. All slices are assumed to have a rigid Gaussian distribution of transverse rms sizes (σ_x, σ_y). The centroid of each slice is treated as a dynamical variable in 6D phase space.

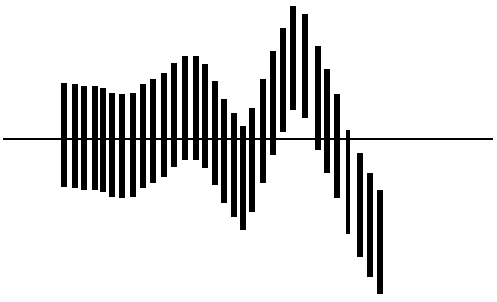

Figure 1: A positron bunch modeled as many longitudinal slices with a rigid transverse Gaussian distribution.

Transversely, we use the 2D vector $\vec{x}_c$ and $\vec{p}_c$ to describe the centroid coordinate and the canonical momentum of the slices. At the beginning of the simulation, all the transverse coordinates and momenta of the slice centroid are set to zero. Longitudinally, the centroid coordinate z and mo-

* Work supported by the Department of Energy under Contract No. DE-AC03-76SF00515

mentum p_z of the slices are initialized to a Gaussian distribution with rms bunch length σ_z and energy spread σ_p respectively.

To speed up the simulation, all electrons are lumped into one single slice at a given azimuthal location s with average β function. This approximation is justified because we know that the head-tail instability is rather insensitive to the location of the impedance. Before the arrival of the positron bunch, the distribution of the electron cloud is re-initialized to a Gaussian distribution with sizes σ_x^e and σ_y^e and the velocities of the electrons are reset to zero. The slices of the bunch are sorted according to their longitudinal positions. Staring with the head, the slices collide with the electron cloud sequentially in time. Under the assumption of a Gaussian distribution, the kick experienced by the i^{th} electron from the electric field of the n^{th} slice is

$$\delta\vec{v_{ei}} = -\frac{2N_b r_e c}{N_s}\vec{F_G}(\vec{x_{ei}} - \vec{x_{cn}}; \vec{\sigma}), \qquad (1)$$

where N_b is the number of positron in a single bunch, r_e is the classical electron radius, c is the speed of light, and $\vec{F_G}$ is given by the Erskine-Bassetti formula [7]. The kick by the electron cloud to the centroid of the slice is expressed as

$$\delta\vec{p_{cn}} = -\frac{2r_e N_e}{N_m\gamma}\sum_{i=1}^{N_m}\vec{F_G}(\vec{x_{cn}} - \vec{x_{ei}}; \vec{\sigma}), \qquad (2)$$

where N_e is the number of electrons and $N_e = 2\pi\sigma_x^e\sigma_y^e C n_e$ for the electron cloud with an initial transverse Gaussian distribution, C is the circumference of the ring, and n_e is the density of the electron cloud. Note that the distribution of the electron cloud is not directly used in the calculation and the expression is based on the conservation of the momentum. The approximation is valid only when the size of the electron cloud is much larger than the size of the beam. Between the collisions of two adjacent slices the electrons drift, $\delta\vec{x_e} = \vec{v_e} * dz/c$, where dz is the longitudinal distance between two slices.

3 LATTICE MAP

To see the dynamical effects of the positron beam, we track the centroid of the slices with its betatron and synchrotron motions. We first transfer the phase-space coordinates to the normalized coordinates with a matrix,

$$A_x^{-1} = \begin{pmatrix} \frac{1}{\sqrt{\beta_x}} & 0 \\ \frac{\alpha_x}{\sqrt{\beta_x}} & \sqrt{\beta_x} \end{pmatrix}, \qquad (3)$$

where β_x and α_x are the Courant-Snyder parameters. Then we perform a rotation and radiation damping on the normalized coordinates by another matrix,

$$R_x = e^{-\frac{1}{\tau_x}}\begin{pmatrix} \cos(2\pi\nu_x) & \sin(2\pi\nu_x) \\ -\sin(2\pi\nu_x) & \cos(2\pi\nu_x) \end{pmatrix}, \qquad (4)$$

where ν_x is the betatron tune and τ_x is damping time in unit of turn. Here we apply the radiation damping on the centroid of slice because the centroid of the beam always damps to a closed orbit while the positions of individual positron will be balanced between the noise of quantum excitation and radiation damping to reach a finite beam size. To apply lattice chromaticity, we simply use $\nu_x = \nu_x^0 + \xi_x p_z$. Finally, we transfer the coordinate back to physical phase space with the inverse of the matrix A_x^{-1},

$$A_x = \begin{pmatrix} \sqrt{\beta_x} & 0 \\ -\frac{\alpha_x}{\sqrt{\beta_x}} & \frac{1}{\sqrt{\beta_x}} \end{pmatrix}. \qquad (5)$$

In the vertical and longitudinal planes, similar formulas are applied. In the longitudinal plane, we have $\beta_z = \sigma_z/\sigma_p$, $\alpha_z = 0$, and $\tau_z = 0$.

4 PARAMETERS

The LER at PEP-II is a positron storage ring. The current operating parameters are tabulated in Table 1. Wiggler magnets in the machine are turned off for higher luminosity. The bunch charge N_b is chosen to correspond to the peak value in regular operation. The vertical emittance is estimated from the luminosity scan. The other parameters are at their design values which are very close to the measured values.

Table 1: Parameters for the LER at PEP-II

Parameter	**Description**	**Value**
E (Gev)	Beam energy	3.1
C (m)	Circumference	2200
N_b	Number of positrons	1.0×10^{11}
β_x (m)	Average horizontal beta	16.52
β_y (m)	Average vertical beta	17.83
τ_t (turn)	Transverse damping time	9740
ϵ_x (nm-rad)	Horizontal emittance	24.0
ϵ_y (nm-rad)	Vertical emittance	1.50
σ_z (cm)	Bunch length	1.30
σ_p	Energy spread	7.7×10^{-4}
ν_x	Horizontal tune	0.649
ν_y	Vertical tune	0.564
ν_s	Synchrotron tune	0.025

The parameters related to the electron cloud are not yet well established. Based on the recent simulation [8] for the generation of an electron cloud, the saturation density is $n_e^s \simeq 2 \times 10^5 \mathrm{cm}^{-3}$. Since we are interested in only the dynamics of the single bunch in this study, the density is an input parameter in the simulation. The transverse rms sizes of the initial electron distribution when the positron bunch arrives are $\sigma_x^e = 6\mathrm{mm}$ and $\sigma_y^e = 3\mathrm{mm}$. These sizes are much larger than the beam sizes and consistent with the shape of the electron cloud when the density is saturated in the cloud generating simulation.

5 THRESHOLD OF THE INSTABILITY

The algorithm outlined in previous sections has been implemented in an object-oriented C++ class library. In the library, the electron cloud and positron bunch are independent objects that can be constructed by the users. There is no limitation on how many objects of cloud or bunch are allowed in the simulation, and clouds can have different parameters as instances of the cloud class. These features provide us with great flexibility to study various phenomena of the electron cloud instability.

In the simulation, we use a thousand slices for the position bunch and ten thousands macro particles for the electron cloud to ensure a reasonable numerical convergence. The chromaticity is set at zero unless we mention the value explicitly.

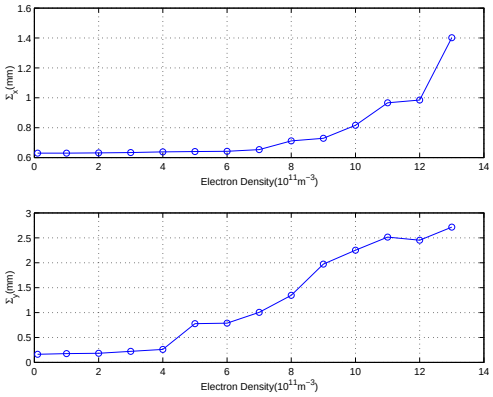

Figure 2: Threshold of head-tail instability caused by electron cloud.

To study the dynamical effects on the positron beam, we vary the density of the electron cloud n_e from 1×10^5 to 1×10^6 cm^{-3}. At each density, we tracked the bunch for 1500 turns. To quantify the emittance growth of the single bunch, we define a projected beam size as $\Sigma_y = \sqrt{\sigma_y^2 + \sigma_y^{c\,2}}$, where σ_y^c is the rms spread of slice centroid. This projected beam size can be measured with a synchrotron light monitor.

The projected beam size at end of the tracking are plotted as a function of the cloud density in Fig. 2. It is clear from the figure that the relative growth of the beam size is much larger in the vertical plane than in the horizontal plane. There is a sudden and huge increase of the beam size in the vertical plane near the density $n_e^{th} = 5 \times 10^5$ cm^{-3}, which we call the threshold of the emittance growth caused by the electron cloud. It will become clear in the next section that it is the also the threshold of the head-tail instability.

Beyond the threshold, the projected beam size becomes much larger than the initial beam size. The increase of emittance significantly reduces the luminosity in the collider and therefore B-factories are limited by this effect in general. Once the instability occurs, the growth time is on the order of the synchrotron period, that is about 40 turns in the simulation. The growth time becomes shorter as the density increases. Below the threshold, there is still sizable growth of the emittance. That will be the subject of a latter section.

6 DIPOLE SPECTRUM AND MODE COUPLING

The head-tail instability can be driven by conventional impedance from the radio-frequency cavities. The effects have been simulated by Myers [9]. For impedance induced by the electron cloud, similar effects should apply. Here we analyze the Fourier spectrum of the beam centroid that is calculated as an average of the slice centroid. The vertical dipole spectra at five different densities below the threshold density n_e^{th} are shown in Fig. 3. We can see from the figure that all modes are shifting upward as the density increases because of the coherent tune shift generated by the electron cloud. Due to the focusing effect of the electron cloud, the modes shift in the opposite direction of its conventional counterpart, in which the zero mode is shifting downward as the impedance increases.

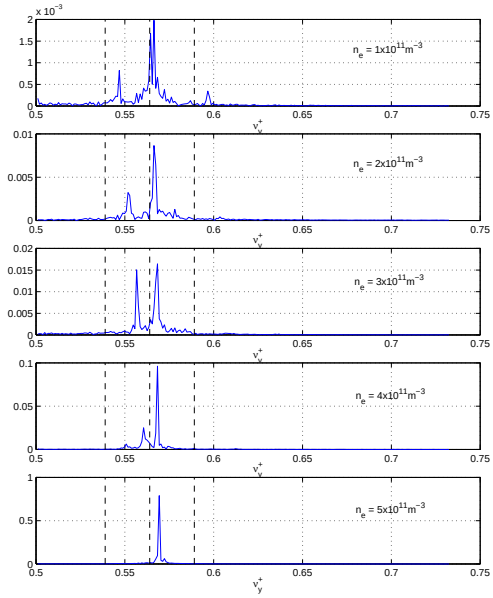

Figure 3: Fourier spectrum of the beam centroid as the density of the electron cloud increases to the threshold. The dashed lines present the betatron tune and synchrotron sidebands.

Since the "$l = -1$" mode, which starts at the lower synchrotron sideband, moves faster than the "$l = 0$" mode starting at the betatron tune, two modes finally merge with each other at the threshold density n_e^{th} as shown in Fig. 3. This behavior is called mode coupling in the literature [10]. The density at which two modes merge is the threshold of the strong head-tail instability. Note that this threshold coincides with the one at which a sudden and huge growth of emittance occurs as we discussed in the last section.

These beam spectra can be measured with a standard spectrum analyzer. The observation of twin peaks that approach each other as the beam current increases is very important experimental evidence to confirm that the head-tail instability is indeed the cause of the single-bunch emittance growth. Since the electron cloud can be generated only when the total beam current is very high and there are many bunches in the ring, the measurement needs to be carried out under the setting of multi-bunch operation although the head-tail instability itself is a single-bunch effect.

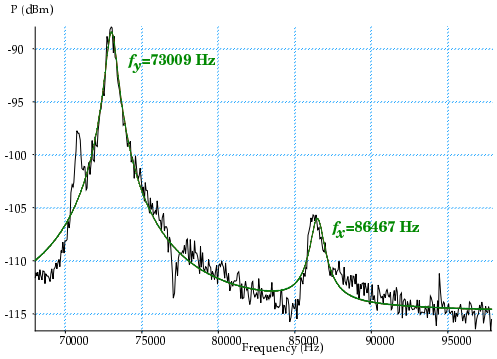

Figure 4: A measurment of the vertical spectrum in the LER with a single beam, 762 bunches with mini gaps and 5% abort gap. The green line is a fit of a double-Lorentzian squared to the data. Squared because this are power spectrum. (Courtesy of Uli Wienands, 2002.)

A measurement of the vertical dipole spectrum at 939mA beam current with bunch spacing $s_b = 8.5\text{ns}$ has been carried out for the LER at PEP-II and shown in Fig. 4. The measured spectrum matches well to the simulated spectrum shown in the first plot in Fig. 3 in terms of the direction and value of the mode shift. The agreement indicates that the electron cloud density is about $n_e \simeq 1 \times 10^5\text{cm}^{-3}$ when the beam current is near 1A in the ring. This density is half of the saturated density in the recent simulation for generating the cloud as we mentioned earlier. The density is also below the threshold density n_e^{th}. The density is about 1% of the average neutralization density $N_b/(\pi h_x h_y L_b)$, where h_x and h_y are the half aperture of the horizontal and vertical chamber respectively, and L_b is the bunch spacing. This ultra low density of the electron cloud near the beam may be attributed to the solenoid winding on the beam pipe.

7 BEAM BLOWUP ALONG A BUNCH TRAIN

In general, when a bunch train is used in the ring, the electron cloud density along the train fits well to the equation

$$n_e(t) = n_e^s[1 - \exp(-t/\tau)], \qquad (6)$$

where τ is the time constant to reach the saturation density n_e^s. For the current operation of the PEP-II, we use a single long train with bunch spacing $s_b = 8.5\text{ns}$ and 5% abort gap. In this bunch pattern, $n_e^s = 2 \times 10^5\text{cm}^{-3}$ and $\tau = 50\text{ns}$ based on the recent simulation [8] for the cloud generation. Clearly, the density in the ring is below the head-tail threshold $n_e^{th} = 5 \times 10^5\text{cm}^{-3}$. However, there is still sizable emittance growth below n_e^{th} as we have noticed in the previous simulation.

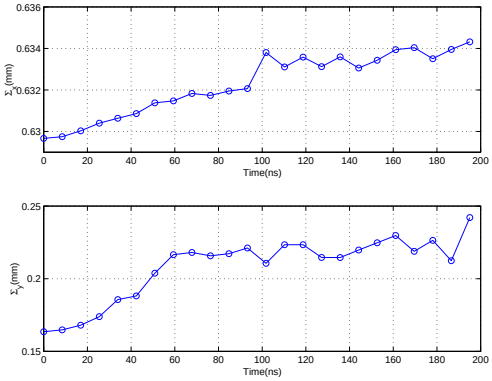

Figure 5: Beam size increase along a bunch train with 8.5ns bunch spacing.

To study in detail the emittance growth below the threshold density, we track the first 20 bunches in the train up to 5000 turns. Each bunch interacts with an electron cloud with the density according to Eqn. 6. The projected beam size at the end of the tracking is shown in Fig. 5. We can see a 30% increase of the vertical beam size along the train. The increase is consistent with the observation seen at KEK-B [3] although the parameters of the rings may differ. It is also consistent with the bunch-by-bunch luminosity measurement [11] at PEP-II. That indicates again, independently, that the density in the ring is quite low compared to the neutralization density.

8 EFFECT OF CHROMATICITY

As we have shown in the simulation, the strong head-tail instability occurs at a threshold density when chromaticity is set at zero. Beyond the threshold, the beam size increases dramatically. The chromaticity is known for stabilizing the conventional head-tail instability. In this section, we will study the effects when the instability is driven by the electron cloud.

We track a bunch through 1500 turns at different vertical chromaticity ranging from -10 to 10 with a fixed density $n_e = 8 \times 10^5\text{cm}^{-3}$ which is above the threshold density n_e^{th}. The turn-by-turn dipole motion of the bunch is plotted in Fig. 6 at three settings of chromaticity: namely +2, 0, and -2. As clearly shown in the figure, the positive chromaticity damps down the unstable motion, the negative chromaticity actually magnifies the motion, and at zero chromaticity, the modulation of synchrotron oscillation stabilizes the motion to a finite amplitude.

The most machines are likely operated with the positive chromaticity that significantly suppresses the dipole motion

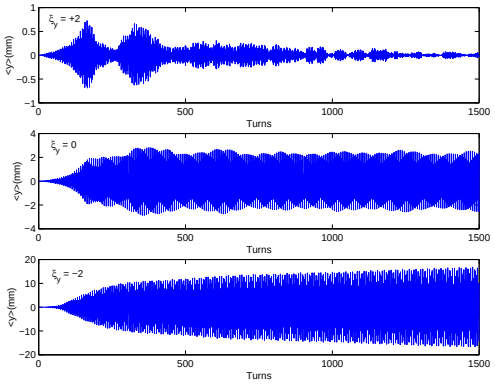

Figure 6: Evolution of beam centroid with three different chromaticities: +2, 0, and -2.

as shown in the simulation. That explains why the mode coupling in the dipole spectrum is so hard to be observed. To make a measurement, one has to set the chromaticity near zero.

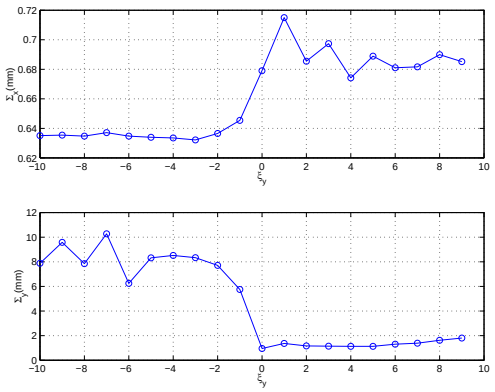

Figure 7: Projected vertical beam size as a function of vertical chromaticity.

The effect of chromaticity on the beam size is shown in Fig. 7. One can see that the positive chromaticity up to 10 units does not change the beam size and the negative one makes a very large blowup in beam size. This behavior is consistent with the experimental observation at PEP-II.

9 SUMMARY

Dynamical interaction between the positron bunch and electron cloud has been simulated in a simple model. We find that the density threshold of the strong head-tail instability is $n_e^{th} \simeq 5\times10^5\mathrm{cm}^{-3}$, which is approximately 5% of the neutralization density. At the threshold, we see the two modes merging into a single mode and a sudden and huge increase of the beam size. Even below the threshold, the beam size still blows up significantly. Based on comparison to experimental observation, we can conclude that the LER at PEP-II is operated (or limited) below the threshold density. The cloud density near the beam is a small percentage of the neutralization density when the ring is operated the regular bunch pattern and beam current.

It is surprising that such a simple model can explain so many experimental observations. In the model, the main mechanism of the beam blowup is explained with the spread of the transverse centroid of the longitudinal slides.

Many additional simulations have been done for the investigation. Here, we will summarize the main results. Although they are many parameters related to the dynamics, the important ones are the beam energy and intensity, bunch length, average beta function, chromaticity, and synchrotron tune. In general, a higher energy, lower beta function, and shorter synchrotron period alleviate the head-tail instability. The positive chromaticity suppresses the unstable dipole motion but has litter effect on the beam size when the density is above the threshold. The Landau damping from the tune spread generated by the second order perturbation of the very strong sextupoles in the ring is not large enough to damp down the instability.

Once the instability starts, we can do little about the vertical blowup of the beam size. The huge emittance growth reduces the single bunch luminosity, limits the total currents in the storage ring, and hence limits the total luminosity.

We have ignored analytical approach to the instability in this paper. The analytical treatment has been covered by Heifets in this proceeding. The wake field for a coasting beam extracted from this code has been compared to his analytical result. The agreement is very good. So we expect similar results can be obtained with analytical estimate.

There is still one of puzzle remained to be resolved: The beam size blowup is also observed in the horizontal plane in PEP-II while the blowup always occurs in the vertical plane in the simulation. One possible explanation for this discrepancy is due to the large coupling that is not yet included in the simulation.

10 ACKNOWLEDGMENTS

I would like to thank M. Furman, S. Heifets, M. Pivi, and J. Seeman for their collaboration. I would also like to thank F.-J. Decker, R. Holtzapple, A. Kulikov, K. Ohmi, and especially U. Wienands for many helpful discussions and sharing the experimental data and NERSC for supercomputer support.

11 REFERENCES

[1] M. Izawa, Y. Sato, and T. Toyomasu, "The Vertical Instability in a Positron Bunched Beam," Phys. Rev. Lett. **74** 5044 (1995).

[2] K. Ohmi, "Beam-Photoelectron Interactions in Positron Storage Rings," Phys. Rev. Lett. **75** 1526 (1995).

[3] H. Fukuma *et al*, "Observation of Vertical Beam Blow-up in KEKB Low Energy Ring," Proc. EPAC, Vienna, Austria, 2000, p. 1124.

[4] A. Kulikov, *et al*, "The Electron Cloud Instability at PEP-II," Proc. PAC, Chicago, 2001, p. 1903.

[5] K. Ohmi and F. Zimmermann, “Head-Tail Instability Caused by Electron Clouds in Positron Rings,” Phys. Rev. Lett. **85** 3821 (2000).

[6] M. A. Furman and G. R. Lambertson, Proc. Intl. Workshop on Multibunch Instabilities in Future Electron and Positron Acceletors(BMI-97), KEK, Tsukuba, Japan, 15-18 July 1997.

[7] M. Bassetti and G. Erskine, CERN ISR TH/80-06 (1980).

[8] M. Pivi, Private communication.

[9] S. Myers, Proc. IEEE Part. Conf., Washingtaon, 1987, p. 503.

[10] A. W. Chao, *Physics of Collective Beam Instabilities in High Energy Accelerators* (Wiley-Interscience Publication, New York, (1993).

[11] F.-J. Decker, *et al*, “Complicated Bunch Pattern in PEP-II,” Proc. PAC, Chicago, 2001, p. 1963.